

ORIGINAL ARTICLE

Spatially-Explicitly Predicting Suitability of Three Apple Diseases in China: A Comparative Analysis of Five Species Distribution Models

Bin Chen¹  | Gang Zhao^{1,2} | Qi Tian³ | Linjia Yao³ | Amit Kumar Srivastava⁴ | Sen Chen³ | Ning Yao⁵ | Liang He⁶ | Qiang Yu²

¹College of Soil and Water Conservation Science and Engineering, Northwest A&F University, Yangling, Shaanxi, China | ²State Key Laboratory of Soil and Water Conservation and Desertification Control, Yangling, Shaanxi, China | ³College of Natural Resources and Environment, Northwest A&F University, Yangling, Shaanxi, China | ⁴Leibniz Centre for Agricultural and Landscape Research (ZALF), Multi-Scale Modelling and Forecasting, Müncheberg, Germany | ⁵College of Water Resources and Architectural Engineering/Key Lab of Agricultural Soil and Water Engineering in Arid and Semiarid Areas, Ministry of Education, Northwest A&F University, Yangling, Shaanxi, China | ⁶National Meteorological Center, Beijing, China

Correspondence: Gang Zhao (gang.zhao@nwafu.edu.cn) | Qiang Yu (yuq@nwafu.edu.cn)

Received: 25 January 2025 | **Revised:** 2 June 2025 | **Accepted:** 30 June 2025

Funding: The authors acknowledge the San qin Scholars Smart Agriculture Innovation Team and the funding by the Key Research and Development Program of Shaanxi (Grant 2023-ZDLNY-64).

Keywords: apple disease | disease management | environment suitability | model ensemble | species distribution models

ABSTRACT

Apple Valsa Canker (AVC), Apple Ring Rot (ARR), and Alternaria Blotch on Apple (ABA) represent major threats to China's apple industry. Understanding the environmental suitability of these diseases is essential for effective orchard management and disease prevention. However, their large-scale spatial distribution and environmental interactions remain insufficiently studied. In this research, we analysed data from 1392 locations using five species distribution models—Generalised Linear Model (GLM), Generalised Additive Model (GAM), Support Vector Machines (SVM), Maximum Entropy (MaxEnt) and Random Forest (RF)—to predict the environmental suitability of these diseases across apple-growing regions in China. Model performance was evaluated using the True Skill Statistic (TSS) and the Area Under the Receiver Operating Characteristic Curve (AUC). MaxEnt and RF consistently outperformed the other models, achieving AUC values above 0.95 and TSS scores exceeding 0.78 for all three diseases. Areas with the highest environmental suitability were primarily located in the Bohai Bay, Loess Plateau and Old Course of the Yellow River regions. Among the environmental variables analysed, the mean temperature of the driest quarter and the annual maximum temperature emerged as the most influential, consistent with the physiological conditions favourable for pathogen development. The key climatic variables identified and their associated disease response curves align with established epidemiological patterns for the three diseases. By integrating ecological insights with predictive modelling, this study provides a robust foundation for targeted disease management and the development of early warning systems under changing climate conditions.

1 | Introduction

Apple (*Malus domestica*) is one of the most widely cultivated and consumed fruits globally. China leads in apple production,

generating approximately 46 million metric tons in 2021, which accounts for over 50% of global production (FAOSTAT 2023). However, the industry faces severe challenges from apple diseases, which threaten both yield and fruit quality. Among

these, Apple Ring Rot (ARR), Apple Valsa Canker (AVC) and Alternaria blotch on Apple (ABA) are the most damaging diseases (Wang et al. 2018). These diseases not only impair tree growth but also drastically reduce yield and market value, causing substantial economic losses (Guo et al. 2009; Hu et al. 2016).

AVC, caused by *Valsa mali*, is a destructive disease that mainly affects tree trunks and branches, causing internal tissue decay, leading to tree decline and eventual death (Chen et al. 2016). ARR, caused by *Botryosphaeria dothidea*, primarily manifests as lesions on fruits and branches, potentially leading to fruit rot and even tree death in severe cases. ABA, a leaf disease caused by *Alternaria mali*, is characterised by brown spots on leaves, which can result in premature leaf fall, thereby impacting photosynthesis and fruit development (Hu et al. 2005). Collectively, these diseases significantly threaten apple orchards by weakening tree vitality and reducing overall yields. To control these diseases, farmers must apply substantial amounts of pesticides, greatly increasing cultivation costs and intensifying the economic burden on growers (Hu et al. 2016; Wang et al. 2018). Addressing their impact is crucial for developing effective management strategies that can enhance apple quality and boost farmers' incomes in China.

The prevalence of the three apple diseases is shaped by a complex interplay of host resistance, pathogen presence, environmental conditions, and management practices (Agrios 2005). Among these factors, environmental conditions play a fundamental role, significantly influencing the occurrence and severity of diseases (Singh et al. 2023). Key variables such as temperature, humidity, and rainfall directly affect the development and spread of these diseases (Hu et al. 2005, 2006; Pan et al. 2012). Understanding the potential geographic distribution of apple diseases by analysing their relationship with environmental factors is crucial for providing timely guidance on field management and surveillance (Xu et al. 2020). However, the spatial relationship between these diseases (ARR, AVC and ABA) and environmental conditions remains inadequately explored.

Recently, species distribution models (SDMs) have emerged as invaluable tools for analysing the relationship between plant diseases and environmental variables, enabling the prediction of disease environment suitability (Zhao et al. 2022). SDMs are widely used to identify areas susceptible to various plant diseases, providing crucial insights for targeted disease management (Xu et al. 2020). These models are generally classified into two categories: correlative and mechanistic. Mechanistic SDMs, also known as process-based or biophysical models, use established equations to simulate species' physiological responses and predict the potential distribution of species (Kearney and Porter 2009). Although these models offer causal explanations, their practical implementation can be complex (Dormann et al. 2012). In contrast, correlative SDMs employ statistical and machine learning techniques to establish relationships between species distribution and environmental factors. Due to their scalability and adaptability, correlative SDMs are widely favoured for predicting how climate affects ecological niches, assessing the impact of biological invasions and supporting conservation and biodiversity efforts (Geary et al. 2022). Increasingly, these models are being used for disease management, particularly in predicting the spread of pests and plant pathogens, making

them essential tools for managing disease outbreaks (Batista et al. 2023; Yoon et al. 2023).

Correlative SDMs have proven invaluable for predicting the spatial distribution of plant diseases; however, their effectiveness can vary significantly depending on the chosen modelling approach. The correlative SDMs are typically categorised into classical regression models and machine learning models. Classical regression models, such as generalised linear models (GLMs) and generalised additive models (GAMs), are widely used due to their simplicity and interpretability (Botella et al. 2018). These models establish relationships between species presence and environmental predictors, offering clear insights into the influence of each variable. However, they often assume linear or additive relationships, which may not fully capture complex ecological interactions. In contrast, machine learning models, such as random forests (RF), support vector machines (SVM), and boosted regression trees (BRT), have gained popularity for their ability to model non-linear relationships and interactions among variables (Guo et al. 2015). These models are particularly adept at handling large datasets and complex environmental factors, providing more flexible and accurate predictions. However, their complexity can lead to overfitting and reduced interpretability, making it challenging to understand the underlying ecological mechanisms (Narouei-Khandan 2014).

The choice of model can significantly influence the predicted distribution of diseases, as different algorithms may yield divergent results when applied to the same dataset (Naimi and Araújo 2016). This discrepancy is a critical issue, as it complicates the decision-making process for disease management. Therefore, a comprehensive comparison of these models is essential to identify the most suitable approach for accurately predicting the potential distribution of fungal pathogens. By analysing the performance of various algorithms under different environmental and geographic conditions, researchers can enhance the reliability of disease assessments and improve management strategies.

In this study, we utilised five widely used species distribution models (SDMs) to predict the environmental suitability for the three major apple diseases in China. The primary objectives were to: (1) compare the predictive performance of the five SDMs, (2) analyse the key environmental factors influencing the occurrence of the three apple diseases and (3) simulate the spatial distribution of these diseases across the main apple-planting regions in China. The outcome of the study will provide insights into predicting the spatial distribution of major apple diseases and inform targeted disease management strategies in China.

2 | Materials and Methods

2.1 | Overall Workflow

Figure 1 outlines the overall workflow of the study, highlighting the key steps in data processing, model evaluation, and post-modelling analysis. The process begins with the selection of 23 climatic and 4 topographic variables, which are refined using the Variance Inflation Factor (VIF) method to reduce multicollinearity, resulting in 14 selected environmental variables. Field

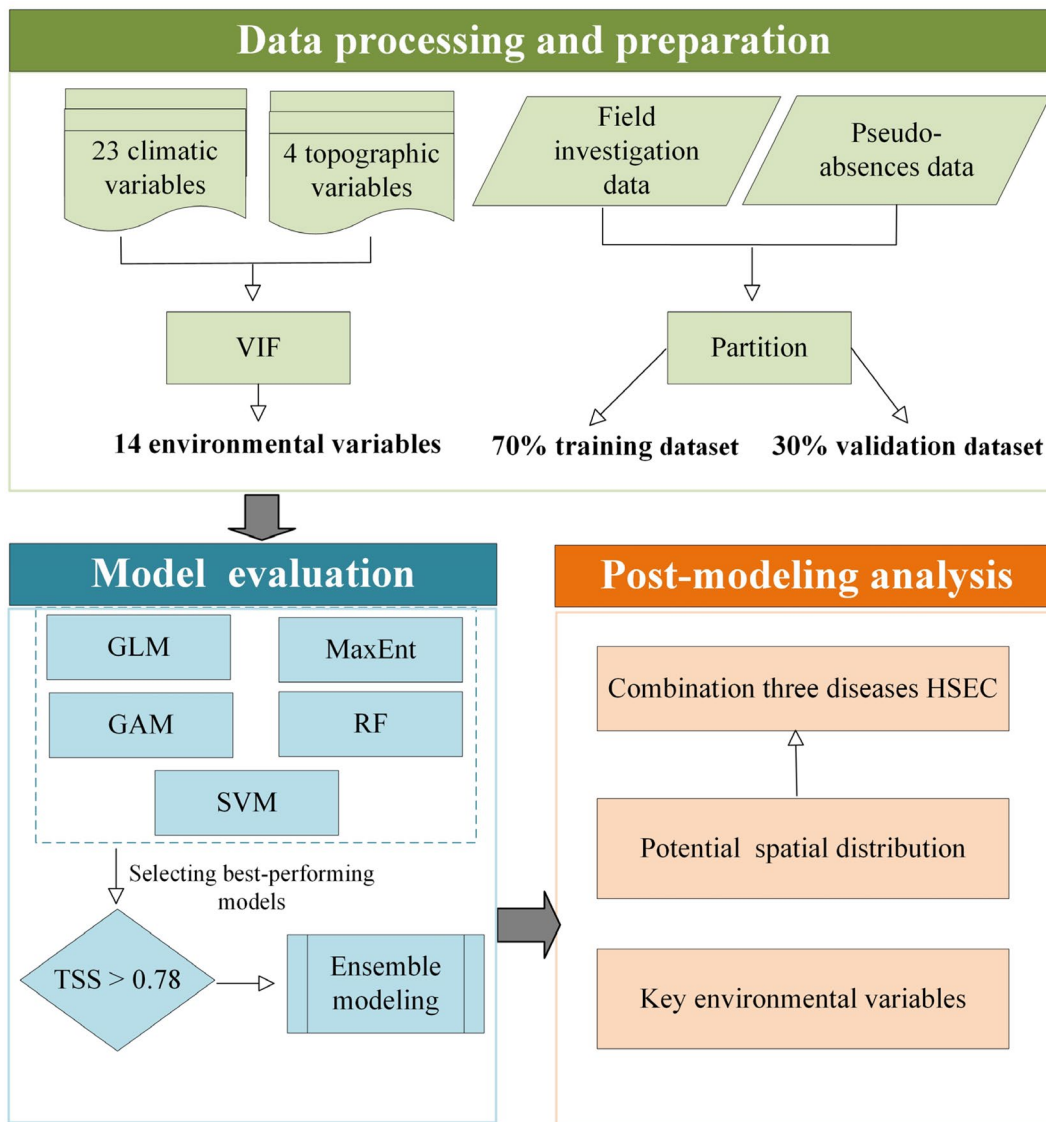


FIGURE 1 | The overall workflow of this study. VIF, variance inflation factor; GLM, Generalised Linear Model; GAM, generalised Additive Model; MaxEnt, Maximal Entropy; RF, Random Forest; SVM, Support Vector Machines; TSS, The True Skill Statistic; HSEC, Highly Suitable Environmental Conditions.

investigation data and pseudo-absence data are then partitioned into a 70% training dataset and a 30% validation dataset. The modelling phase involves evaluating five species distribution models: Generalised Linear Model (GLM), Generalised Additive Model (GAM), Maximal Entropy (MaxEnt), Random Forest (RF) and Support Vector Machines (SVM). Models achieving a True Skill Statistic (TSS) > 0.78 are chosen for ensemble modeling. In the post-modelling analysis, the results are integrated to identify key environmental variables, project the potential spatial distribution of the three major apple diseases, and determine the combination of highly suitable environmental conditions.

2.2 | Study Area

Apples are cultivated across diverse regions in China with diverse climatic conditions. According to Qu and Zhou (2016), there are five apple cultivation regions in China, namely the Loess Plateau (provinces including Shaanxi, Gansu, Shanxi and

Ningxia), Bohai Bay (Shandong, Hebei, Liaoning, Beijing and Tianjin), the Old Course of the Yellow River (Henan, Jiangsu and Anhui), the cold Southwestern Highlands (Yunnan, Sichuan and Guizhou), and Xinjiang region. The climate characteristics of these regions are summarised in Table S1. Only a small amount of apple trees was cultivated in Tibet, Inner Mongolia, northeast, and the southern regions, which are referred to as “Other regions” in this study. As a result, we make use of six apple cultivation regions in this study (Figure S1a). Among them, the Bohai Bay and the Loess Plateau have the biggest cultivation area and highest production (Figure S1b,c). In 2019, the total orchard area of these two regions was 1.55 million ha and production was 33.77 million metric ton, 78.2% and 79.6% of the national total, respectively. The highest unit yield is from the Old Course of the Yellow River (Figure S1d). It is worth noting that due to the current lack of a comprehensive dataset on apple orchard distribution in China, we did not apply land use data to mask out non-orchard areas in the study. Moreover, modelling suitability of apple diseases in regions not currently under

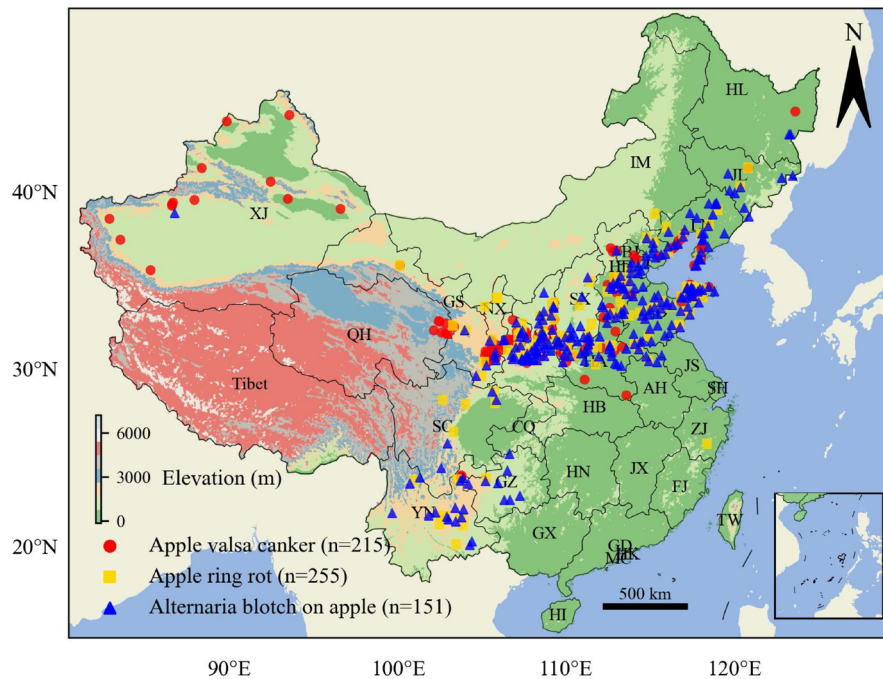


FIGURE 2 | Observed presence points of Apple Valsa Canker, Apple Ring Rot and Alternaria Blotch on Apple in China, with 215, 255 and 151 points recorded for each disease, respectively. GX, Guangxi; FJ, Fujian; GZ, Guizhou; YN, Yunnan; JX, Jiangxi; HN, Hunan; ZJ, Zhejiang; SH, Shanghai; CQ, Chongqing; HB, Hubei; SC, Sichuan; AH, Anhui; JS, Jiangsu; HA, Henan; Tibet, Tibet; SD, Shandong; QH, Qinghai; NX, Ningxia; SN, Shaanxi; TJ, Tianjin; SX, Shanxi; BJ, Beijing; HE, Hebei; GS, Gansu; LN, Liaoning; JL, Jilin; XJ, Xinjiang; IM, Inner Mongolia; HL, Heilongjiang; HK, Hong Kong; MC, Macao; HI, Hainan; GD, Guangdong; TW, Taiwan.

cultivation is also meaningful for informing future expansion and planning of apple production areas.

2.3 | Presence and Absence Data

Presence data for the three apple diseases were sourced from orchard surveys, the National Public Data Channel of Apple Big Data (<https://appledata-channel.agri.cn/>), and published literature. The orchard survey and published literature data were based on field investigations conducted by plant pathology experts. The public database records were obtained from reports issued by local government plant protection departments, which are based on field-confirmed observations. In all cases, a presence point represents a confirmed occurrence of the disease, defined as the field detection of visible disease symptoms under local environmental conditions.

To ensure data accuracy, geographic coordinates were verified and corrected using Google Earth. A total of 1392 presence points were compiled: 802 for Apple Valsa Canker (AVC), 297 for Apple Ring Rot (ARR) and 293 for Alternaria Blotch on Apple (ABA). To reduce spatial autocorrelation, the dataset was filtered using the ‘spThin’ R package, maintaining a minimum distance of 5 km between records (Mi et al. 2023; Xu et al. 2020). This process yielded 215 records for AVC, 255 for ARR and 151 for ABA (Figure 2).

For absence points, we generated pseudo-absence data using a random spatial sampling method, following the approach used in recent studies (Batista et al. 2023; Ganglo 2023; Mi et al. 2023).

Barbet-Massin et al. (2012) demonstrated that when the number of presence points is relatively low and regression-based modelling techniques are employed—such as GLM or GAM—the use of a large number of pseudo-absences (e.g., 10,000) can help reduce model bias. In this study, this condition applies, as all three apple diseases had a limited number of presence records and the modelling framework included regression-based approaches. Therefore, we randomly generated 1000 pseudo-absence points for each disease using the ‘gRandom’ function in the ‘sdm’ R package (Ganglo 2023).

To further support transparency and reproducibility in our research, we have shared the data and corresponding codes on GitHub at ‘<https://github.com/SmartAG-NWAFU/AppleDiseaseSDM/>’.

2.4 | Environmental Data

In species distribution modelling, the selection of environmental variables is a key factor influencing model accuracy. Most studies primarily utilise bioclimatic variables, such as those provided by the WorldClim database. These variables represent biologically meaningful climatic patterns, including annual averages (e.g., temperature and precipitation), seasonal variability, and climate extremes (e.g., temperature of the coldest/warmest months, and precipitation of the wettest/driest quarters) (Bai et al. 2022; Booth 2018; Booth et al. 2014; Fick and Hijmans 2017; Puchałka et al. 2023). In this study, we incorporated these standard 19 bioclimatic variables (Bio1–Bio19). However, the focal organisms in our research

TABLE 1 | Environmental variables used in predicting the potential distribution of Apple Valsa Canker, Apple Ring Rot and Alternaria Blotch on Apple in China.

Type	Variables	Meaning	Units	Description
Climate variables	Bio2	Mean diurnal range	°C	$\sum_{1}^{12} \frac{T_{\max} - T_{\min}}{12}$
	Bio3	Isothermality		$\frac{\text{Bio2}}{\text{Bio7}} \times 100$
	Bio4	Temperature seasonality		$\text{Std}(\bar{T}_1^{12}) \times 100$
	Bio8	Mean temperature of the wettest quarter	°C	Mean temperature of the 3 wettest months
	Bio9	Mean temperature of the driest quarter	°C	Mean temperature of the 3 driest months
	Bio13	Precipitation of the wettest month	mm	Precipitation of the 3 wettest month
	Bio15	Precipitation seasonality		$\frac{\text{Std}_p}{\text{Mean}_p} \times 100$
	Bio19	Precipitation of the coldest quarter	mm	Precipitation the of the coldest 3 months
	T_{\max}	Annual mean maximum temperature	°C	$\sum_{1}^{12} \frac{T_{\max}}{12}$
	Wind	Annual mean surface wind speed at 10 m	$m \times s^{-1}$	$\sum_{1}^{12} \frac{\bar{W}}{12}$
	Relative Humidity	Annual mean relative humidity	$\sum_{1}^{12} \frac{rh}{12}$	
Topographic variables	Aspect	Aspect		
	Slope	Slope	Degree	
	Curvature	Curvature		

Note: \bar{T} is mean monthly temperature, \bar{P} is mean monthly precipitations, \bar{W} is mean monthly surface wind speed, rh is mean monthly relative humidity, T_{\max} is maximum temperature of month, T_{\min} is minimum temperature of a month, and a quarter is 3 months (1/4 of the year).

are plant pathogenic fungi, which exhibit distinct physiological requirements. Previous studies have demonstrated that certain meteorological factors—such as wind speed and relative humidity—play critical roles in pathogen dispersal and successful host infection (Hu et al. 2006; Wang et al. 2018). To capture these dynamics, we included four additional climate variables: minimum temperature, maximum temperature, relative humidity, and surface wind speed.

Moreover, topographic features can influence microclimates and pathogen distribution (Xu et al. 2020). Therefore, we incorporated four topographic variables: elevation, slope, aspect, and curvature. Based on this rationale, our model utilised a total of 27 environmental variables—comprising 19 bioclimatic, four key climate, and four topographic variables (Table S2).

Bioclimatic and temperature variables were sourced from WorldClim version 2.1 at a spatial resolution of 2.5 arc-min. Relative humidity and surface wind speed data were obtained from the Loess Plateau Sub-Center of the National Earth System Science Data Center (<http://loess.geodata.cn>), originally at a 1 km resolution. Topographic variables were derived from a digital elevation model (DEM) provided by the Data Center for Resources and Environmental Sciences (<http://www.resdc.cn>), with slope, aspect, and curvature calculated using ArcGIS 10.2 (ESRI, Redlands, CA, USA). To ensure consistency, all raster

layers were resampled and reprojected to 2.5 arc-min using the ‘raster’ package in R. Administrative boundary data for China were obtained from the National Basic Geographic Information Center (<http://www.ngcc.cn>).

2.5 | Species Distribution Models

To identify suitable areas for three apple diseases, SDMs were employed as a robust framework for linking environmental factors to disease occurrence. Five widely used SDMs were trained and compared for three apple diseases. The models included GLM, GAM, MaxEnt, RF and SVM (Table S3).

Prior to model fitting, correlation coefficients among the variables were calculated (Figure S2) to identify highly correlated pairs (correlation coefficient > 0.9). The variable with the highest variance inflation factor (VIF) was excluded from each correlated pair, and this process was repeated until no strongly correlated pairs remained (Naimi and Araújo 2016). This selection process resulted in 14 environmental variables (Table 1) being chosen as inputs for the models.

To enhance model evaluation, a cross-validation (2-fold with 10 replicates) was performed. In training and testing, 70% of the data were used as a training dataset, and the remaining 30% were used

for evaluation. We utilised true skill statistics (TSS, Equation (1)) and the area under the receiver operating characteristic curve (AUC, Equation (2)) to assess the performance of models. TSS and AUC are widely used and complementary evaluation metrics that quantify a model's discriminatory capacity in distinguishing between species presence and absence (Chen et al. 2025; Jiang et al. 2022). The TSS ranges from -1 to 1 , where values greater than 0.7 are generally indicative of high predictive accuracy and robust model performance (Gong et al. 2020). The AUC ranges from 0.5 (no better than random prediction) to 1 (perfect discrimination), with values exceeding 0.8 typically reflecting strong model reliability in predicting species distributions (Gong et al. 2020).

$$\begin{cases} \text{TPR} = \frac{\text{TP}}{\text{TP} + \text{FN}} \\ \text{TNR} = \frac{\text{TN}}{\text{FP} + \text{TN}} \\ \text{TSS} = \text{TPR} + \text{TNR} - 1 \end{cases} \quad (1)$$

where TP, FN, FP and TN are true positive, false negative, false positive, and true negative cases predicted by the models under a given threshold, respectively. TPR and TNR were sensitivity and specificity.

$$\begin{cases} \text{AUC} = 1 - \frac{1}{m^+ \times m^-} \sum_{x^+ \in D^+} \sum_{x^- \in D^-} (W(f(x^+) - f(x^-))) \\ W(f(x^+) - f(x^-)) = 1, f(x^+) \geq f(x^-) \\ W(f(x^+) - f(x^-)) = 0, f(x^+) < f(x^-) \end{cases} \quad (2)$$

where, m^+ and m^- were sample size marked as 1 and 0; D^+ and D^- were the sets marked as 1 and 0; x^+ and x^- were the sample marked as 1 and 0; $f(x^+)$ and $f(x^-)$ were the model predicted values under a given threshold.

2.6 | Ensemble Modelling and Projection

After evaluating the performance of five SDMs, we selected the two best-performing models, MaxEnt and RF, to create ensemble models. The SDMs predicted the survival probability or potential distribution of the three diseases, with values ranging from 0 to 1 for each pixel. To distinguish suitable from unsuitable areas, we applied the threshold that maximises the True Skill Statistic (TSS) for each disease model (Batista et al. 2023; Mi et al. 2016). The resulting thresholds (T) were 0.184 for AVC, 0.211 for ARR, and 0.186 for ABA. Areas with predicted suitability values below T were classified as unsuitable. For values $\geq T$, we further divided the range $[T, 1]$ into three equal intervals using the breakpoints $T + (1 - T)/3$ and $T + 2 \times (1 - T)/3$. This method allowed each disease to maintain its specific suitability threshold while ensuring a consistent classification scheme across models. The final classification included four categories: unsuitable environmental conditions (USEC), low suitability (LSEC), moderate suitability (MSEC) and high suitability (HSEC). The classification intervals are detailed in Table S4.

To assess the relative importance of environmental variables, we evaluated the correlation between predicted values and model outputs after variable permutation using the 'getVarImp' function in the 'sdm' package in R (Naimi and Araújo 2016). The

mean relative importance of each environmental variable was calculated, weighting the contribution of each model by its TSS performance. Furthermore, we examined the relationship between the predicted occurrence probability of diseases and four key environmental variables using marginal response curves. These curves demonstrate how the predicted probability depends on a single variable while holding all others constant.

Highly suitable environmental conditions indicate areas with an elevated likelihood of disease occurrence and potential outbreaks (Iloldi-Rangel et al. 2012). Mapping these high-risk zones is critical for informed orchard management and disease prevention strategies. To evaluate the spatial overlap of highly suitable areas for the three apple diseases, we developed the Combined Highly Suitable Index (CHS). The CHS is a composite index generated by overlaying the binary highly suitability maps for each disease—AVC, ARR and ABA (see Equation (3)).

$$\text{CHS} = \text{HAVC} \times 1 + \text{HARR} \times 2 + \text{HABA} \times 4 \quad (3)$$

where HAVC, HARR, and HABA represent the highly suitable environmental conditions and other conditions of Apple Valsa Canker, Apple Ring Rot, and Alternaria Blotch on Apple in the binary image, and the values correspond to 1 and 0, respectively.

This encoding yields CHS values ranging from 0 to 7, representing all possible combinations of high suitability across the three diseases. This approach facilitates the identification and visualisation of multi-disease hotspots. Similar overlay techniques have been used in ecological risk assessments and multi-species distribution studies to delineate areas of compounded risk or conservation priority (e.g., Mustikaningrum et al. 2023; Rana et al. 2025; Tempa and Yuden 2023). The interpretation of CHS categories is detailed in Table 2.

TABLE 2 | The combination of highly suitable environmental conditions for Apple valsa canker, Apple ring rot and Alternaria Blotch on Apple.

CHS	Description
0	None of the diseases (Apple Valsa Canker, Apple Ring Rot or Alternaria Blotch) have highly suitable conditions
1	Only Apple Valsa Canker has highly suitable conditions (HAVC)
2	Only Apple Ring Rot has highly suitable conditions (HARR)
3	Apple Valsa Canker and Apple Ring Rot have highly suitable conditions (HAVC-HARR)
4	Only Alternaria Blotch has highly suitable conditions (HABA)
5	Apple Valsa Canker and Alternaria Blotch on Apple have highly suitable conditions (HAVC-HABA)
6	Alternaria Blotch and Apple Ring Rot have highly suitable conditions (HARR-HABA)
7	Highly suitable conditions for all three diseases (HAVC-HARR-HABA)

3 | Results

3.1 | SDMs Performance

As shown in Figure 3, MaxEnt and RF exhibited significantly superior performance compared to the other three models. In terms of the TSS, both MaxEnt and RF achieved the highest scores (≥ 0.78) across all three apple diseases, whereas SVM (≥ 0.72), GLM (≥ 0.69) and GAM (≥ 0.69) demonstrated comparatively lower performance. A similar pattern was observed for the AUC, with MaxEnt and RF consistently attaining the highest values (≥ 0.95), followed by SVM (≥ 0.92), GLM (≥ 0.90) and GAM (≥ 0.88). These findings suggest that MaxEnt and RF offer enhanced reliability and predictive accuracy for disease suitability modelling relative to the other models evaluated.

3.2 | Variability in Predicted Spatial Distributions

The spatial distribution of the three apple diseases simulated by the five models exhibited notable differences (Figure 4). Among the models, the GLM predictions deviated the most from those of the other four models, while the SVM predictions showed inconsistencies with the actual occurrence points in certain areas. MaxEnt and RF models exhibit a high degree of consistency, with the average absolute difference in predicted suitability values remaining below 1.3% throughout the study area (see Figures S5–S7).

Specially, for AVC, the GLM model predicted that highly suitable environmental conditions (HSEC) were primarily concentrated in Shaanxi and Sichuan provinces. In contrast, the other four models identified HSEC mainly in the Loess Plateau region of Shaanxi Province. In Xinjiang, the SVM model predicted only a small area of low-suitability environmental conditions (LSEC), whereas the other models predicted areas with moderately suitable environmental conditions (MSEC) and HSEC. For ARR and ABA, the GLM model showed a strip-like distribution of HSEC extending

from Hainan, Guangxi, Sichuan, Shaanxi, Henan, Shandong, to Hebei provinces. However, the other four models revealed a more localised distribution. For ARR, HSEC was mainly concentrated in Shaanxi, Henan, Shanxi, Shandong and Hebei provinces. Similarly, for ABA, HSEC was primarily distributed in Shaanxi, Shanxi, Henan and Shandong provinces. Furthermore, in the SVM predictions, few or no suitable areas for ARR and ABA were identified in Sichuan, Yunnan and Guizhou provinces, despite a significant number of occurrence points in these regions.

3.3 | Key Environmental Variables Driving Disease Distribution

The importance of environmental variables in determining the occurrence of the three apple diseases is illustrated in Figure S3. The results highlight the critical role of temperature-related variables, including the mean temperature of the driest quarter (Bio9) and the average of the annual mean maximum (Tmax). Precipitation variables, such as precipitation of the wettest month (Bio13) and precipitation of the coldest quarter (Bio19), as well as relative humidity, were also shown to be key factors influencing the spatial distribution of AVC, ARR and ABA.

The marginal response curves illustrating the relationships between the probability of disease presence and four key environmental variables are shown in Figure 5. ARR and ABA exhibited similar responses to the environmental variables compared to AVC. Specifically, for Tmax (annual mean maximum temperature), the probability of occurrence for all three diseases increased gradually as Tmax rose from 0°C to 10°C. For AVC, the occurrence probability stabilised as Tmax reached 15°C, whereas higher Tmax values (up to 30°C) favoured the development of ARR and ABA. Regarding Bio13 (precipitation sum of the wettest month), AVC showed low sensitivity, with its presence probability remaining consistently low (< 0.2) regardless of

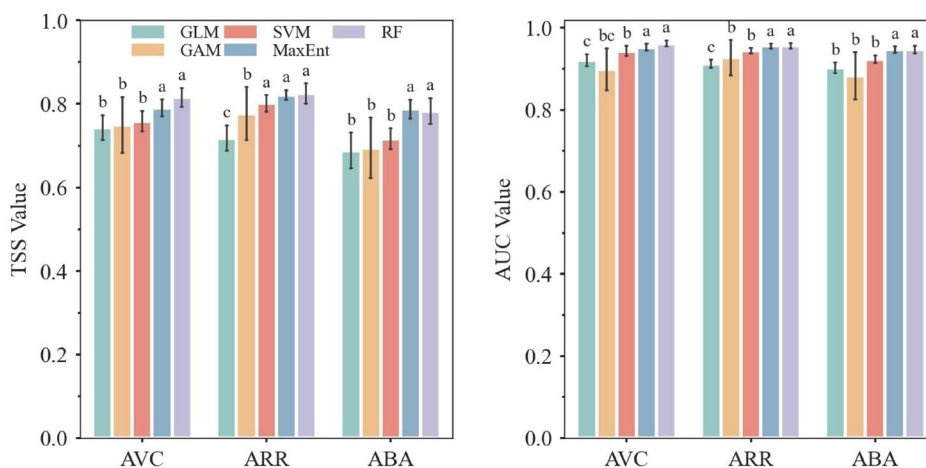


FIGURE 3 | The area under the receiver operating characteristic curve (AUC) and true skill statistic (TSS) values for five species distribution models in predicting the potential distribution of Apple Valsa Canker (AVC), Apple Ring Rot (ARR) and Alternaria Blotch on Apple (ABA). Different lowercase letters indicate significant differences in performance metrics among modelling methods under the same apple disease ($p < 0.05$). Error bars represent standard deviations. Model performance was classified based on commonly used thresholds: for AUC, values ≥ 0.9 indicate excellent performance, 0.8–0.9 indicate good performance, 0.7–0.8 indicate fair performance and < 0.7 indicate poor performance; for TSS, values ≥ 0.8 are considered excellent, 0.7–0.8 good, 0.4–0.7 fair and < 0.4 poor (Gong et al. 2020; Jiang et al. 2022).

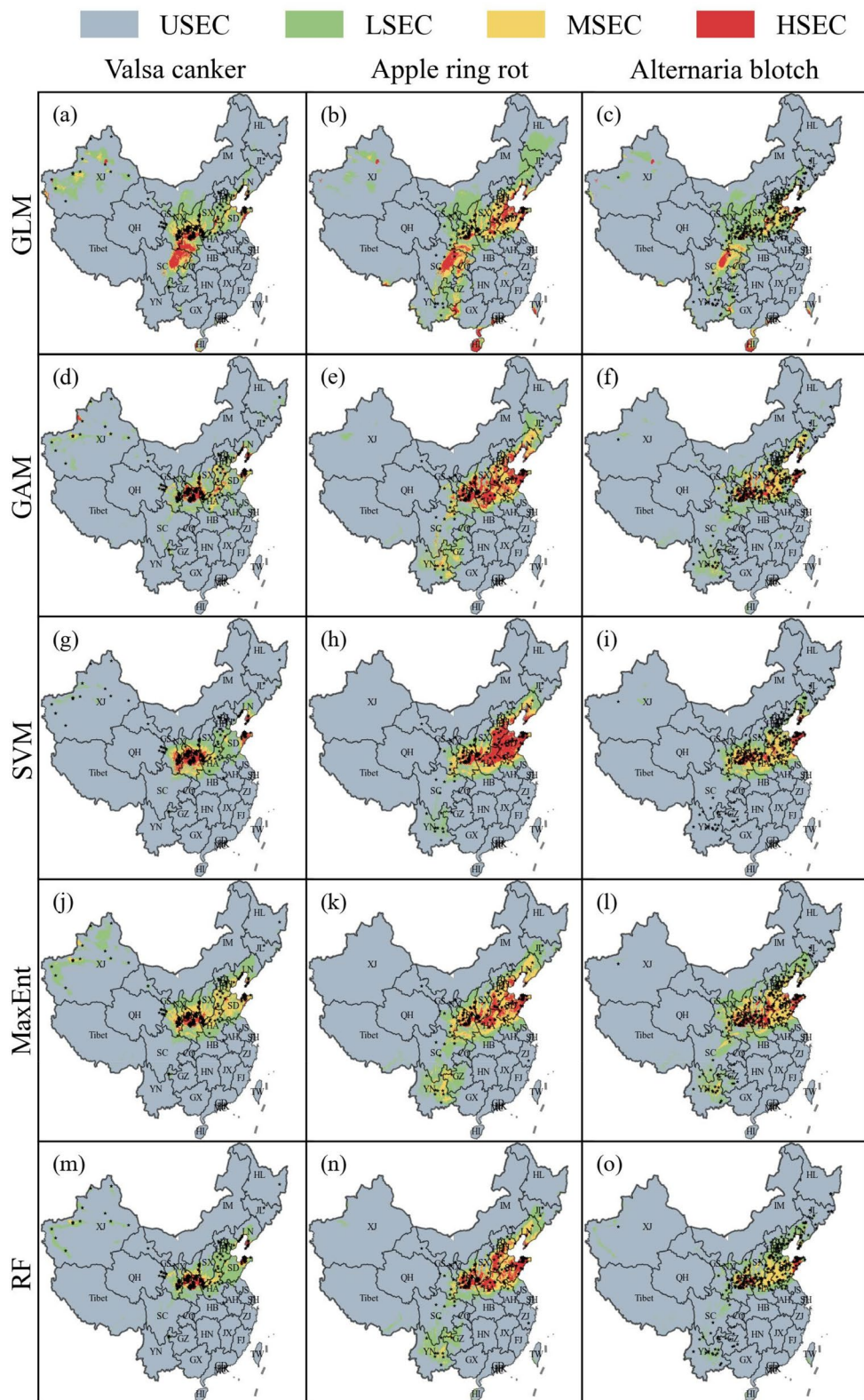


FIGURE 4 | The potential distribution of three apple diseases (Apple Valsa Canker, Apple Ring Rot and Alternaria Blotch on Apple) estimated using five species distribution models (GLM, GAM, SVM, MaxEnt and RF) in China, and the small black dot represents the presence points of the three diseases. The suitability levels include unsuitable environmental conditions (USEC), low-suitability environmental conditions (LSEC), moderately suitable environmental conditions (MSEC) and highly suitable environmental conditions (HSEC). GX, Guangxi; FJ, Fujian; GZ, Guizhou; YN, Yunnan; JX, Jiangxi; HN, Hunan; ZJ, Zhejiang; SH, Shanghai; CQ, Chongqing; HB, Hubei; SC, Sichuan; AH, Anhui; JS, Jiangsu; HA, Henan; Tibet, Tibet; SD, Shandong; QH, Qinghai; NX, Ningxia; SN, Shaanxi; TJ, Tianjin; SX, Shanxi; BJ, Beijing; HE, Hebei; GS, Gansu; LN, Liaoning; JL, Jilin; XJ, Xinjiang; IM, Inner Mongolia; HL, Heilongjiang; HK, Hong Kong; MC, Macao; HI, Hainan; GD, Guangdong; TW, Taiwan.

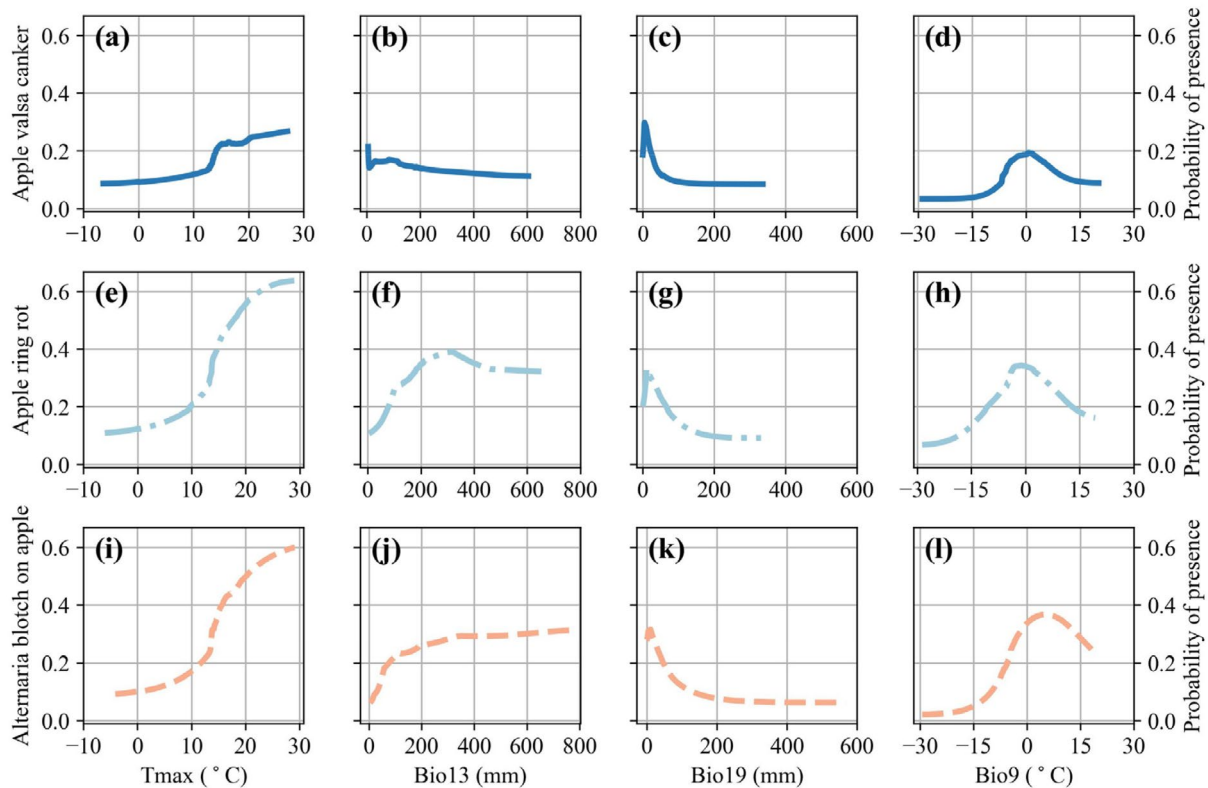


FIGURE 5 | Response curves showing the relationship between the predicted suitability of the three apple diseases—Apple Valsa Canker, Apple Ring Rot, and Alternaria Blotch on Apple—and the four most influential environmental variables. Tmax: Annual mean maximum temperature (°C); Bio13: Precipitation of the wettest month (mm); Bio19: Precipitation of the coldest quarter (mm); Bio9: Mean temperature of the driest quarter (°C).

Bio13 values. In contrast, the presence probability of ARR increased with Bio13, reaching a peak at approximately 300 mm. Beyond this threshold, higher Bio13 values strongly promoted the presence of ABA. For Bio19 (precipitation of the coldest quarter), the presence probabilities of all three diseases decreased rapidly once Bio19 exceeded 0 mm, indicating a negative correlation with cold-season precipitation. The response curves for Bio9 (mean temperature of the driest quarter) displayed a distinct peak for all three diseases. Their presence probabilities gradually increased as temperatures rose to approximately -15°C , peaked around 0°C , and then declined gradually as temperatures increased further.

3.4 | Potential Distribution of Diseases

ARR had the highest total area of suitability and highly suitable environmental conditions (HSEC), followed by ABA and AVC (Figure 6d). The HSEC of AVC was primarily distributed in Shaanxi, Gansu, and Shanxi provinces (Figure 6a). For ARR, the HSEC was predominantly concentrated in Shaanxi, Shanxi, Henan, Hebei, Shandong, and Liaoning provinces (Figure 6b). The spatial distribution of ABA and ARR exhibited similarities, as did their responses to the primary environmental variables (Figure 5).

The HSEC of ABA was predominantly concentrated in Shaanxi, Shanxi, Henan, Hebei and Shandong provinces (Figure 6c). Specifically, we observed the presence of AVC's low-suitability environmental conditions (LSEC) and moderately suitable

environmental conditions (MSEC) in northern Xinjiang, while the other two diseases had minimal suitability zones in that region. In contrast to the other two diseases, widespread LSEC and MSEC of ARR were also observed in Jilin province and the border areas of Yunnan, Guizhou and Guangxi provinces. Additionally, the HSEC associated with ARR exhibited a broad distribution across the provinces of Shandong and Hebei provinces.

3.5 | Combination of HSEC for Diseases

Figure 7 shows the spatial distribution of highly suitable environmental conditions (HSEC) for the three apple diseases. These areas were primarily concentrated in the Bohai Bay region ($209.4 \times 10^3 \text{ km}^2$), the Loess Plateau ($155.6 \times 10^3 \text{ km}^2$), and the old river course of the Yellow River ($56.3 \times 10^3 \text{ km}^2$). The overlapping HSEC for all three diseases—AVC, ARR, and ABA—were mainly located in the Loess Plateau ($52.9 \times 10^3 \text{ km}^2$) and the Bohai Bay ($14.4 \times 10^3 \text{ km}^2$), accounting for 77.9% and 21.2% of the total overlapping area, respectively. Among the pairwise combinations, the joint HSEC for ARR and ABA (HARR-HABA) covered the largest area, totalling $57.9 \times 10^3 \text{ km}^2$, with major concentrations in the Bohai Bay. Regarding individual diseases, ARR exhibited the widest HSEC ($230.9 \times 10^3 \text{ km}^2$), followed by AVC ($35.8 \times 10^3 \text{ km}^2$) and ABA ($1.62 \times 10^3 \text{ km}^2$). Notably, the HARR in the Bohai Bay region accounted for 69.0% of the total area. Similarly, the HAVC in the Loess Plateau reached $33.9 \times 10^3 \text{ km}^2$, representing 94.8% of the total area.

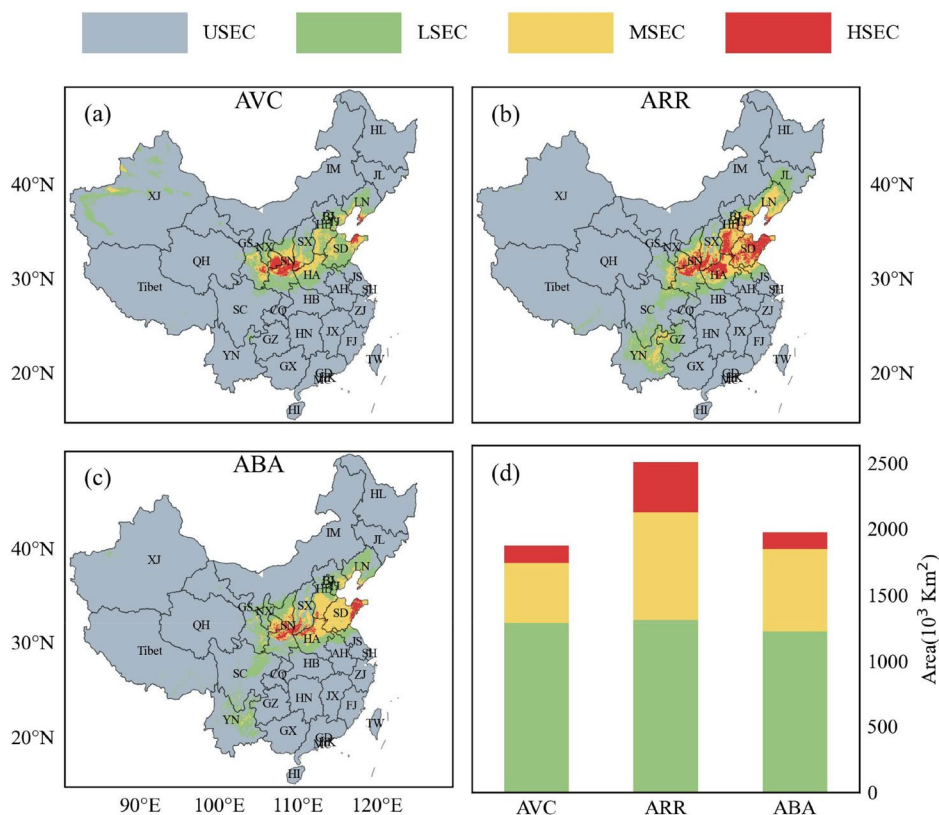


FIGURE 6 | Predicted spatial distribution (a–c) and areas of different suitability levels (d) of Apple Valsa Canker (AVC), Apple Ring Rot (ARR) and Alternaria Blotch on Apple (ABA). The suitability levels include unsuitable environmental conditions (USEC), low-suitability environmental conditions (LSEC), moderately suitable environmental conditions (MSEC), and highly suitable environmental conditions (HSEC). GX, Guangxi; FJ, Fujian; GZ, Guizhou; YN, Yunnan; JX, Jiangxi; HN, Hunan; ZJ, Zhejiang; SH, Shanghai; CQ, Chongqing; HB, Hubei; SC, Sichuan; AH, Anhui; JS, Jiangsu; HA, Henan; Tibet, Tibet; SD, Shandong; QH, Qinghai; NX, Ningxia; SN, Shaanxi; TJ, Tianjin; SX, Shanxi; BJ, Beijing; HE, Hebei; GS, Gansu; LN, Liaoning; JL, Jilin; XJ, Xinjiang; IM, Inner Mongolia; HL, Heilongjiang; HK, Hong Kong; MC, Macao; HI, Hainan; GD, Guangdong; TW, Taiwan.

4 | Discussion

Apple Valsa Canker, Apple Ring Rot and Alternaria Blotch on Apple are the most important diseases that severely impact apple production in China, leading to a significant economic loss for fruit growers (Wang et al. 2018). To effectively prevent and control these diseases, it is crucial to understand the key environmental factors that influence their occurrence and accurately map their potential distribution areas (Kumar et al. 2016). This study conducted extensive data collection on disease occurrences and environmental variables related to these three diseases. We found Maximal Entropy and Random Forest are the two best-performing models in disease suitability environment prediction, and the two models' ensemble was used to predict spatial distributions. The mapped hotspots of the diseases' suitability levels and hotspots can guide the design of disease management measures.

4.1 | Performances of the Five SDMs

The five SDMs exhibited notable differences in their ability to simulate the potential distribution of apple diseases (Figures 3 and 4). These disparities emphasise the importance of addressing model-related uncertainty when applying SDMs to disease suitability predictions. In this study, MaxEnt and RF consistently outperformed

the other models. As shown in Figure 3, both MaxEnt and RF achieved the highest performance across all three apple diseases in terms of TSS and AUC. Specifically, MaxEnt and RF yielded average TSS values of ≥ 0.78 , significantly higher than those of SVM (≥ 0.72), GLM (≥ 0.69) and GAM (≥ 0.69) ($p < 0.05$). A similar trend was observed for AUC, with MaxEnt and RF reaching values of ≥ 0.95 , also significantly outperforming SVM (≥ 0.92), GLM (≥ 0.90) and GAM (≥ 0.88) ($p < 0.05$). These results indicate that MaxEnt and RF provided significantly better predictive accuracy compared to the other models evaluated in this study.

Our findings are consistent with previous studies. For instance, Elith et al. (2006) demonstrated that MaxEnt outperformed GLM and GAM in predicting the distributions of 226 species using 16 different modelling algorithms. Ganglo (2023) also reported higher AUC values for MaxEnt (0.84) and RF (0.86) compared to GLM (0.81) and GAM (0.83). Furthermore, Yates et al. (2018) noted that GLM and GAM tend to produce unrealistic predictions when extrapolated beyond the range of training data—an issue also reflected in our results.

Model selection should therefore be undertaken with caution. While MaxEnt has frequently been favoured for its high predictive accuracy (Li, Fan, et al. 2020), other studies have found that RF can outperform MaxEnt under specific conditions (Mi

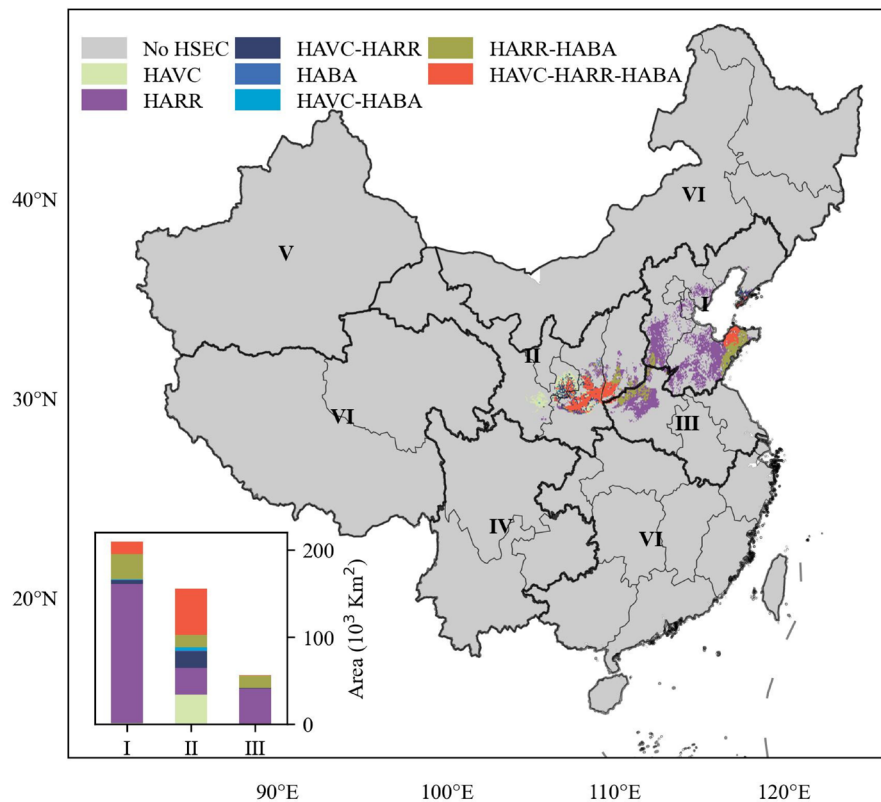


FIGURE 7 | Distribution of highly suitable environmental conditions (HSEC) and corresponding areas for three major apple diseases—Apple Valsa Canker (AVC), Apple Ring Rot (ARR) and Alternaria Blotch on Apple (ABA)—across key apple-planting regions in China. Regions I–VI represent: I—Bohai Bay, II—Loess Plateau, III—Old Course of the Yellow River, IV—Cold Southwestern Highlands, V—Xinjiang and VI—Other apple-planting regions. The legend includes the following HSEC combinations: No HSEC: Areas without highly suitable environmental conditions for any of the three diseases; HAVC: HSEC for AVC only; HARR: HSEC for ARR only; HABA: HSEC for ABA only; HAVC–HARR: Overlapping HSEC for AVC and ARR; HAVC–HABA: Overlapping HSEC for AVC and ABA; HARR–HABA: Overlapping HSEC for ARR and ABA; HAVC–HARR–HABA: Overlapping HSEC for all three diseases.

et al. 2017). These variations may be attributed to differences in species' ecological characteristics, environmental predictor suitability, and modelling strategies (Stoklosa et al. 2015). Additionally, Norberg et al. (2019), in a large-scale comparative study involving 33 SDMs, emphasised that model performance is highly task-specific. They advocated for the use of a limited number of models with complementary strengths, recommending either the best-performing model or an ensemble approach for more reliable predictions.

In light of these findings, we emphasise the necessity of rigorous model validation and careful selection of SDMs. Choosing the most appropriate individual model—or combining complementary models—can significantly enhance the reliability of spatial predictions and support more effective strategies for disease risk assessment and management.

4.2 | Impact of Environmental Variables on Diseases Suitability

Understanding the relationship between disease occurrences and environmental variables is essential for elucidating the mechanisms underlying differences in model predictions (Li, Fan, et al. 2020). Previous studies have identified temperature,

precipitation, relative humidity, and wind speed as the dominant climatic factors influencing the spatial distribution of plant diseases (Yoon et al. 2023). Our findings align with these observations, highlighting temperature variables (Bio9, Tmax), precipitation variables (Bio13, Bio19), and relative humidity as the key drivers of the distribution of the three pathogens. Xu et al. (2020) previously reported that climatic factors exert a stronger influence on the distribution of *Valsa mali* compared to topographic factors, with temperature variables being more impactful than precipitation variables. Our results further corroborate these findings, demonstrating that temperature plays a critical role in determining the distribution of the three pathogens (Figure S3). Additionally, we compared the responses of the three diseases to environmental variables with the optimal environmental conditions reported in the literature. For example, the occurrence probability of AVC stabilised when Tmax (annual mean maximum temperature) reached approximately 15°C, whereas higher Tmax values (up to 30°C) were favourable for the development of ARR and ABA (Figure 5).

These findings are consistent with the optimum temperature ranges reported in Table S5: –10°C to 10°C for AVC, 10°C to 40°C for ARR, and 25°C–30°C for ABA. Furthermore, Figure 5 shows that AVC is relatively insensitive to Bio13 (precipitation

sum of the wettest month), while ARR and ABA exhibit their highest occurrence probabilities in regions where Bio13 exceeds 200 mm. Table S5 also indicates that the modes of propagation differ among the diseases: AVC primarily spreads through pruning wounds, whereas ARR and ABA are primarily dispersed by wind and rain. These differences in propagation mechanisms likely contribute to the varying sensitivities of the diseases to precipitation. Specifically, the higher demand for Bio13 in ARR and ABA may be explained by their dependence on rain-splash and wind for pathogen dispersal.

Besides climatic and topographic variables, other environmental factors such as soil moisture may also influence host resistance and pathogen development. The variations in soil moisture can affect the physiological condition of host plants, potentially altering their susceptibility to pathogens (Garrett et al. 2006; Qiao et al. 2022). Additionally, soil water availability can influence microbial communities and disease dynamics in the rhizosphere (van Bruggen and Semenov 2000). However, due to the complexity of these interactions and limited mechanistic understanding, soil moisture was not included in this study. Future studies incorporating soil-related variables may further enhance the accuracy and ecological relevance of disease risk models.

This study primarily focuses on environmental variables; however, it is important to acknowledge the potential influence of additional factors such as orchard management practices and host susceptibility. Interventions like fungicide application, pruning, and irrigation can significantly influence disease dynamics (Zaller et al. 2023). Likewise, the regional variability in apple cultivar susceptibility may also play a critical role in disease occurrence. These factors were not included in the current analysis due to the lack of standardised, region-specific data on orchard practices and cultivar resistance. Future research should prioritise the collection and integration of such data to enhance the accuracy and biological relevance of disease risk modelling.

4.3 | Potential Spatial Distribution of Diseases

AVC, ARR and ABA have long posed significant risks to the apple industry in China (Li et al. 2013). For example, Hu et al. (2016) found that these three diseases are causing more yield and quality losses compared to other apple diseases (e.g., Marssonina blotch and Fruit spot) with a nationwide survey. They pointed out that the Bohai Bay and Loess Plateau, two major apple-producing regions in China, have consistently been heavily affected by these three diseases. Xu et al. (2020) also found that the suitability zone of AVC is primarily concentrated in Bohai Bay and Loess Plateau. Comparing these findings, we revealed that AVC and ABA primarily exhibit low to moderate suitability, whereas ARR shows moderate to high suitability in Bohai Bay and Loess Plateau (Figure S4). Additionally, we also found that ARR and AVC have dominant distributions in the cold Southwestern Highlands and Xinjiang regions, respectively, but their suitability is mainly low to moderate (Figure 6, Figure S4). This may be closely related to the climate characteristics of the apple production regions and the environmental suitability of the corresponding fungal pathogens. Xinjiang, for example, has an average annual temperature of 7°C–10°C and an average annual rainfall of only 100–300 mm (Table S1). The

optimal temperature range for AVC aligns with these conditions (–10°C to 10°C), and it is not sensitive to rainfall variables (Figure 5), making Xinjiang an environmentally suitable zone for the AVC pathogen (*Valsa mali*). The same applies to ARR in the cold Southwestern Highlands, where the higher average annual temperature and abundant annual rainfall provide a potentially favourable environment for the survival of the ARR pathogen (*Botryosphaeria dothidea*).

Therefore, we recommend prioritising disease prevention and control efforts for these three diseases in the Bohai Bay and Loess Plateau, which are the two major apple-producing regions in China. However, it is important to note that the spatial distribution of the three diseases is uneven across different production regions. Hence, disease management should be tailored according to the local environmental conditions and the suitability levels in each specific region.

4.4 | Implications of Disease Suitability Mapping for Apple Cultivation Management

This study reveals the spatial distribution of suitable environmental conditions for three major apple diseases—AVC, ARR and ABA. These mapped hotspots serve as valuable decision-support tools for growers and agricultural authorities, enabling more precise and proactive disease management planning.

In AVC-prone areas, particularly the Loess Plateau, the maps underscore the importance of routine trunk inspections, early detection of cankers and timely wound treatment to limit disease spread and severity (Zhao et al. 2022). In Bohai Bay, a consistent hotspot for ARR, the maps support the adoption of preventive measures, including scheduled pruning, improved orchard ventilation, and real-time moisture monitoring to reduce the environmental factors that favour fungal outbreaks (Ramírez-Gil et al. 2021). In regions where all three diseases are likely to co-occur (HAVC–HARR–HABA), a comprehensive approach is essential. Growers are encouraged to implement integrated disease management practices, such as crop rotation with non-host species, targeted fungicide applications, canopy thinning to reduce humidity, and the use of resistant cultivars (Cabrefiga et al. 2023). These maps can guide the allocation of resources for frequent disease scouting, deployment of weather-based forecasting systems, and investment in precision agriculture technologies (e.g., remote sensing and sensor-based monitoring) to facilitate early warning and site-specific interventions.

Moreover, the suitability maps are valuable for long-term orchard planning, helping producers avoid planting in high-risk zones or adjust planting densities and row orientations to reduce disease transmission. They can also inform policy development, directing regional extension efforts and financial support programmes toward areas facing the highest combined disease pressures.

4.5 | Limitations and Future Work

While this study leveraged a large disease occurrence dataset and addressed key sources of model-related uncertainty, several

limitations remain. First, the modelling framework primarily focused on climatic and topographic variables, excluding potentially important factors such as population density, land use, apple tree age, and soil nutrient status (Peng et al. 2016). For example, we were unable to incorporate land use layers due to the unavailability of high-resolution, spatially explicit data on apple cultivation across China. Similarly, varietal resistance was not explicitly modelled. The spatial distribution of resistant versus susceptible apple cultivars can significantly influence disease occurrence patterns and may introduce bias into presence/absence data. However, comprehensive maps of cultivar deployment are currently lacking, limiting the integration of this critical variable. Future research should prioritise the development and incorporation of cultivar-specific resistance data to enhance the biological accuracy of disease distribution models. Second, although we applied a variable selection procedure to reduce multicollinearity among predictors, this process inevitably excluded some environmental variables that may still hold ecological relevance for pathogen distribution (Narouei-Khandan 2014). Future work could explore dimensionality reduction techniques or hierarchical modelling frameworks that retain ecological complexity while minimising statistical redundancy. Third, while broad-scale precipitation indicators offer valuable insights into climatic suitability, they may not fully capture the short-term microclimatic conditions (e.g., daily rainfall events, transient humidity peaks) that are critical for pathogen infection and disease progression. Incorporating higher-resolution temporal climate and disease survey data, where available, would likely improve model precision.

Finally, it is important to note that the models developed in this study predict environmental suitability for disease occurrence, rather than actual outbreak risk. Suitability reflects the presence of favourable conditions for pathogen survival, but does not account for key on-the-ground factors such as host availability, cultivar susceptibility, or orchard management practices. To move towards more comprehensive assessments of disease risk, future studies should aim to integrate environmental, biological, and management datasets within a unified modelling framework. This interdisciplinary approach would allow for more accurate forecasting and better-informed disease prevention strategies, particularly under dynamic climate conditions.

5 | Conclusion

This study evaluated the performance of five species distribution models to predict the potential spatial distribution of three major apple diseases in China: Apple Valsa Canker (AVC), Apple Ring Rot (ARR), and Apple Bitter Rot (ABA). Among these models, Maximum Entropy and Random Forest consistently outperformed the others. Our results identified the Bohai Bay region, the Loess Plateau, and the old river course of the Yellow River as key hotspots for the potential distribution of all three diseases. Of the three, ARR showed the largest total area of environmental suitability, particularly in regions with high disease risk.

By aligning predicted disease hotspots with key apple-producing regions, this study provides a scalable framework for prioritising disease surveillance, optimising resource allocation, and guiding orchard planning in the face of increasing

climatic and biotic stress. These insights are especially valuable for informing integrated disease management strategies and supporting long-term orchard planning—enabling growers to avoid high-risk zones or adapt planting densities and row orientations to mitigate disease transmission. As environmental and production conditions continue to shift, tools like these will be essential for enhancing the resilience and sustainability of China's apple industry through informed and forward-looking interventions.

Author Contributions

Bin Chen: conceptualisation, formal analysis, methodology, software, visualisation, writing – original draft. **Gang Zhao:** conceptualisation, supervision, formal analysis, writing – original draft. **Qi Tian:** formal analysis, investigation. **Linjia Yao:** investigation. **Amit Kumar Srivastava:** writing – review and editing. **Sen Chen:** writing – review and editing. **Ning Yao:** writing – review and editing. **Liang He:** writing – review and editing. **Qiang Yu:** supervision, writing – review and editing.

Acknowledgements

The authors acknowledge the San qin Scholars Smart Agriculture Innovation Team and the funding by the Key Research and Development Program of Shaanxi (Grant 2023-ZDLNY-64). The authors also acknowledge the funding by the German Federal Ministry of Education and Research (BMBF) in the framework of the funding measure 'Soil as a Sustainable Resource for the Bioeconomy—BonaRes', project BonaRes (Module A): BonaRes Center for Soil Research, subproject 'Sustainable Subsoil Management—Soil3' (Grant 031B0151A), and partially funded by the Deutsche Forschungsgemeinschaft (DFG, German Research Foundation) under Germany's Excellence Strategy—EXC 2070—390732324. We also extend our appreciation to the two anonymous reviewers, whose thoughtful comments greatly improved the manuscript.

Conflicts of Interest

The authors declare no conflicts of interest.

Data Availability Statement

The data that support the findings of this study are available on request from the corresponding author. The data are not publicly available due to privacy or ethical restrictions.

Peer Review

The peer review history for this article is available at <https://www.webofscience.com/api/gateway/wos/peer-review/10.1111/jph.70123>.

References

- Agrios, G. N. 2005. *Plant Pathology*. 5th ed. Elsevier. <https://doi.org/10.1016/C2009-0-02037-6>.
- Bai, R., J. Wang, and N. Li. 2022. "Climate Change Increases the Suitable Area and Suitability Degree of Rubber Tree Powdery Mildew in China." *Industrial Crops and Products* 189: 115888. <https://doi.org/10.1016/j.indcrop.2022.115888>.
- Barbet-Massin, M., F. Jiguet, C. H. Albert, and W. Thuiller. 2012. "Selecting Pseudo-Absences for Species Distribution Models: How, Where and How Many?: How to Use Pseudo-Absences in Niche Modelling?" *Methods in Ecology and Evolution* 3: 327–338. <https://doi.org/10.1111/j.2041-210X.2011.00172.x>.
- Batista, E., A. Lopes, P. Miranda, and A. Alves. 2023. "Can Species Distribution Models Be Used for Risk Assessment Analyses of Fungal

- Plant Pathogens? A Case Study With Three Botryosphaeriaceae Species." *European Journal of Plant Pathology* 165: 41–56. <https://doi.org/10.1007/s10658-022-02587-7>.
- Booth, T. H. 2018. "Why Understanding the Pioneering and Continuing Contributions of BIOCLIM to Species Distribution Modelling Is Important." *Austral Ecology* 43: 852–860. <https://doi.org/10.1111/aec.12628>.
- Booth, T. H., H. A. Nix, J. R. Busby, and M. F. Hutchinson. 2014. "Bioclim: The First Species Distribution Modelling Package, Its Early Applications and Relevance to Most Current MaxEnt Studies." *Diversity and Distributions* 20: 1–9. <https://doi.org/10.1111/ddi.12144>.
- Botella, C., A. Joly, P. Bonnet, P. Monestiez, and F. Munoz. 2018. "Species Distribution Modeling Based on the Automated Identification of Citizen Observations." *Applications in Plant Sciences* 6: e1029. <https://doi.org/10.1002/aps3.1029>.
- Cabrefiga, J., M. V. Salomon, and P. Vilardell. 2023. "Improvement of Alternaria Leaf Blotch and Fruit Spot of Apple Control Through the Management of Primary Inoculum." *Microorganisms* 11: 101. <https://doi.org/10.3390/microorganisms11010101>.
- Chen, B., G. Zhao, Q. Tian, et al. 2025. "Climate-Driven Shifts in Suitable Areas of Alternaria Leaf Blotch (*Alternaria mali* Roberts) on Apples: Projections and Uncertainty Analysis in China." *Agricultural and Forest Meteorology* 364: 110464. <https://doi.org/10.1016/j.agrfor.2025.110464>.
- Chen, C., B.-H. Li, X.-L. Dong, C.-X. Wang, S. Lian, and W.-X. Liang. 2016. "Effects of Temperature, Humidity, and Wound Age on Valsa Mali Infection of Apple Shoot Pruning Wounds." *Plant Disease* 100: 2394–2401. <https://doi.org/10.1094/PDIS-05-16-0625-RE>.
- Dormann, C. F., S. J. Schymanski, J. Cabral, et al. 2012. "Correlation and Process in Species Distribution Models: Bridging a Dichotomy." *Journal of Biogeography* 39: 2119–2131. <https://doi.org/10.1111/j.1365-2699.2011.02659.x>.
- Elith, J., H. Graham, R. Anderson, M. Dudík, and S. Ferrier. 2006. "Novel Methods Improve Prediction of Species' Distributions From Occurrence Data." *Ecography* 29: 129–151. <https://doi.org/10.1111/j.2006.0906-7590.04596.x>.
- FAOSTAT. 2023. "Apple Production by Area Worldwide." <http://www.fao.org/faostat/en/#data/QCL/visualize>.
- Fick, S. E., and R. J. Hijmans. 2017. "WorldClim 2: New 1-Km Spatial Resolution Climate Surfaces for Global Land Areas." *International Journal of Climatology* 37: 4302–4315. <https://doi.org/10.1002/joc.5086>.
- Ganglo, J. C. 2023. "Ecological Niche Model Transferability of the White Star Apple (*Chrysophyllum albidum* G. Don) in the Context of Climate and Global Changes." *Scientific Reports* 13: 2430. <https://doi.org/10.1038/s41598-023-29048-3>.
- Garrett, K. A., S. P. Dendy, E. E. Frank, M. N. Rouse, and S. E. Travers. 2006. "Climate Change Effects on Plant Disease: Genomes to Ecosystems." *Annual Review of Phytopathology* 44: 489–509. <https://doi.org/10.1146/annurev.phyto.44.070505.143420>.
- Geary, W. L., A. Buchan, T. Allen, et al. 2022. "Responding to the Biodiversity Impacts of a Megafire: A Case Study From South-Eastern Australia's Black Summer." *Diversity and Distributions* 28: 463–478. <https://doi.org/10.1111/ddi.13292>.
- Gong, X., Y. Chen, T. Wang, X. Jiang, X. Hu, and J. Feng. 2020. "Double-Edged Effects of Climate Change on Plant Invasions: Ecological Niche Modeling Global Distributions of Two Invasive Alien Plants." *Science of the Total Environment* 740: 139933. <https://doi.org/10.1016/j.scitotenv.2020.139933>.
- Guo, C., S. Lek, S. Ye, W. Li, J. Liu, and Z. Li. 2015. "Uncertainty in Ensemble Modelling of Large-Scale Species Distribution: Effects From Species Characteristics and Model Techniques." *Ecological Modelling* 306: 67–75. <https://doi.org/10.1016/j.ecolmodel.2014.08.002>.
- Guo, L., J. Li, B. Li, et al. 2009. "Investigations on the Occurrence and Chemical Control of Botryosphaeria Canker of Apple in China." *Plant Protection* 35: 120–123. <https://doi.org/10.3969/j.issn.0529-1542.2009.04.027>.
- Hu, H. T., C. K. Cao KeQiang, W. S. Wang ShuTong, and Z. W. Zhen WenChao. 2005. "Study on the Main Factor for the Epidemic of Alternaria Blotch on Apple."
- Hu, Q. Y., T. L. Hu, Y. N. Wang, S. T. Wang, and K. Q. Cao. 2016. "Survey on the Occurrence and Distribution of Apple Diseases in China." *Plant Protection* 42: 175–179. <https://doi.org/10.3969/j.issn.0529-1542.2016.01.032>.
- Hu, T., S. Wang, P. Song, F. Zhang, W. Zhen, and K. Cao. 2006. "Primary Study on the Crucial Weather Conditions of Mass Infection of Alternaria Mali on Apple." *Journal of Agricultural University of Hebei* 29: 63–66.
- Illoldi-Rangel, P., C.-L. Rivaldi, B. Sissel, et al. 2012. "Species Distribution Models and Ecological Suitability Analysis for Potential Tick Vectors of Lyme Disease in Mexico." *Journal of Tropical Medicine* 2012: 959101. <https://doi.org/10.1155/2012/959101>.
- Jiang, T., B. Wang, X. Xu, et al. 2022. "Identifying Sources of Uncertainty in Wheat Production Projections With Consideration of Crop Climatic Suitability Under Future Climate." *Agricultural and Forest Meteorology* 319: 108933. <https://doi.org/10.1016/j.agrformet.2022.108933>.
- Kearney, M., and W. Porter. 2009. "Mechanistic Niche Modelling: Combining Physiological and Spatial Data to Predict Species' Ranges." *Ecology Letters* 12: 334–350. <https://doi.org/10.1111/j.1461-0248.2008.01277.x>.
- Kumar, S., W. L. Yee, and L. G. Neven. 2016. "Mapping Global Potential Risk of Establishment of *Rhagoletis pomonella* (Diptera: Tephritidae) Using MaxEnt and CLIMEX Niche Models." *Journal of Economic Entomology* 109: 2043–2053. <https://doi.org/10.1093/jee/tow166>.
- Li, B. H., C. X. Wang, and X. L. Dong. 2013. "Research Progress in Apple Diseases and Problems in the Disease Management in China." *Plant Protection* 39: 46–54. <https://doi.org/10.3969/j.issn.0529-1542.2013.05.007>.
- Li, J., G. Fan, and Y. He. 2020. "Predicting the Current and Future Distribution of Three Coptis Herbs in China Under Climate Change Conditions, Using the MaxEnt Model and Chemical Analysis." *Science of the Total Environment* 698: 134141. <https://doi.org/10.1016/j.scitotenv.2019.134141>.
- Mi, C., H. Falk, and Y. Guo. 2016. "Climate Envelope Predictions Indicate an Enlarged Suitable Wintering Distribution for Great Bustards (*Otis tarda dybowskii*) in China for the 21st Century." *PeerJ* 4: e1630. <https://doi.org/10.7717/peerj.1630>.
- Mi, C., F. Huettmann, Y. Guo, X. Han, and L. Wen. 2017. "Why Choose Random Forest to Predict Rare Species Distribution With Few Samples in Large Undersampled Areas? Three Asian Crane Species Models Provide Supporting Evidence." *PeerJ* 5: e2849. <https://doi.org/10.7717/peerj.2849>.
- Mi, C., L. Ma, M. Yang, et al. 2023. "Global Protected Areas as Refuges for Amphibians and Reptiles Under Climate Change." *Nature Communications* 14: 1389. <https://doi.org/10.1038/s41467-023-36987-y>.
- Mustikaningrum, M., A. F. Widhatama, K. W. Widantara, et al. 2023. "Multi-Hazard Analysis in Gunungkidul Regency Using Spatial Multi-Criteria Evaluation." *Forum Geografi* 37, no. 1: 35–45. <https://doi.org/10.23917/forgeo.v37i1.19041>.
- Naimi, B., and M. B. Araújo. 2016. "Sdm: A Reproducible and Extensible R Platform for Species Distribution Modelling." *Ecography* 39: 368–375. <https://doi.org/10.1111/ecog.01881>.
- Narouei-Khandan, H. A. 2014. "Ensemble Models to Assess the Risk of Exotic Plant Pathogens in a Changing Climate (PhD Thesis). Lincoln University."

- Norberg, A., N. Abrego, F. G. Blanchet, et al. 2019. "A Comprehensive Evaluation of Predictive Performance of 33 Species Distribution Models at Species and Community Levels." *Ecological Monographs* 89: e01370. <https://doi.org/10.1002/ecm.1370>.
- Pan, Y., z. Huang, and y. Ma. 2012. "Prediction of Potential Distribution of *Alternaria Mali* Roberts Based on Eaxent Ecological Niche Model 30." <https://doi.org/10.13989/j.cnki.0517-6611.2012.30.207>.
- Peng, H. X., X. Y. Wei, Y. X. Xiao, et al. 2016. "Management of Valsa Canker on Apple With Adjustments to Potassium Nutrition." *Plant Disease* 100: 884–889. <https://doi.org/10.1094/PDIS-09-15-0970-RE>.
- Puchałka, R., S. Paż-Dyderska, A. M. Jagodziński, et al. 2023. "Predicted Range Shifts of Alien Tree Species in Europe." *Agricultural and Forest Meteorology* 341: 109650. <https://doi.org/10.1016/j.agrformet.2023.109650>.
- Qiao, L., X. Wang, P. Smith, et al. 2022. "Soil Quality Both Increases Crop Production and Improves Resilience to Climate Change." *Nature Climate Change* 12: 574–580. <https://doi.org/10.1038/s41558-022-01376-8>.
- Qu, Z., and G. Zhou. 2016. "Possible Impact of Climate Change on the Quality of Apples From the Major Producing Areas of China." *Atmosphere* 7: 113. <https://doi.org/10.3390/atmos7090113>.
- Ramírez-Gil, J. G., J. G. Morales-Osorio, and A. T. Peterson. 2021. "The Distribution of *Phytophthora Cinnamomi* in the Americas Is Related to Its Main Host (*Persea americana*), but With High Potential for Expansion." *Phytopathologia Mediterranea* 60: 521–534. <https://doi.org/10.36253/phyto-12327>.
- Rana, S. K., J. Lindstrom, M. A. Lehrer, M. Ahlering, and J. Hamilton. 2025. "Forecasting Hotspots of Climatic Suitability for Grassland Restoration Under Climate Change in North America." *Biological Conservation* 302: 110988. <https://doi.org/10.1016/j.biocon.2025.110988>.
- Singh, B. K., M. Delgado-Baquerizo, E. Egidi, et al. 2023. "Climate Change Impacts on Plant Pathogens, Food Security and Paths Forward." *Nature Reviews. Microbiology* 21: 640–656. <https://doi.org/10.1038/s41579-023-00900-7>.
- Stoklosa, J., C. Daly, S. D. Foster, M. B. Ashcroft, and D. I. Warton. 2015. "A Climate of Uncertainty: Accounting for Error in Climate Variables for Species Distribution Models." *Methods in Ecology and Evolution* 6: 412–423. <https://doi.org/10.1111/2041-210X.12217>.
- Tempa, K., and K. Yuden. 2023. "Multi-Hazard Zoning for National Scale Population Risk Mapping: A Pilot Study in Bhutan Himalaya." *Geoenvironmental Disasters* 10: 7. <https://doi.org/10.1186/s40677-023-00239-4>.
- van Bruggen, A. H. C., and A. M. Semenov. 2000. "In Search of Biological Indicators for Soil Health and Disease Suppression." *Applied Soil Ecology* 15: 13–24. [https://doi.org/10.1016/S0929-1393\(00\)00068-8](https://doi.org/10.1016/S0929-1393(00)00068-8).
- Wang, S. T., Y. N. Wang, and K. Q. Cao. 2018. "Occurrence of and Research Progress in Important Apple Diseases in China in Recent Years." *Plant Protection* 44: 13–25.
- Xu, W., H. Sun, J. Jin, and J. Cheng. 2020. "Predicting the Potential Distribution of Apple Canker Pathogen (*Valsa Mali*) in China Under Climate Change." *Forests* 11: 1126. <https://doi.org/10.3390/f11111126>.
- Yates, K. L., P. J. Bouchet, M. J. Caley, et al. 2018. "Outstanding Challenges in the Transferability of Ecological Models." *Trends in Ecology & Evolution* 33: 790–802. <https://doi.org/10.1016/j.tree.2018.08.001>.
- Yoon, S., J.-M. Jung, J. Hwang, Y. Park, and W.-H. Lee. 2023. "Ensemble Evaluation of the Spatial Distribution of Pine Wilt Disease Mediated by Insect Vectors in South Korea." *Forest Ecology and Management* 529: 120677. <https://doi.org/10.1016/j.foreco.2022.120677>.
- Zaller, J. G., A. Oswald, M. Wildenberg, et al. 2023. "Potential to Reduce Pesticides in Intensive Apple Production Through Management Practices Could Be Challenged by Climatic Extremes." *Science of the Total Environment* 872: 162237. <https://doi.org/10.1016/j.scitotenv.2023.162237>.
- Zhao, H., X. Xian, Z. Zhao, G. Zhang, W. Liu, and F. Wan. 2022. "Climate Change Increases the Expansion Risk of *Helicoverpa zea* in China According to Potential Geographical Distribution Estimation." *Insects* 13: 79. <https://doi.org/10.3390/insects13010079>.

Supporting Information

Additional supporting information can be found online in the Supporting Information section.